Universal Role of Discrete Acoustic Phonons in the Low-Temperature Optical Emission of Colloidal Quantum Dots

Dan Oron,[1] Assaf Aharoni,[2] Celso de Mello Donega,[3] Jos van Rijssel,[3] Andries Meijerink,[3] and Uri Banin[2,*]

[1]*Department of Physics of Complex Systems, Weizmann Institute of Science, Rehovot, Israel*

[2]*Department of Chemical Physics and Institute for Nanoscience and Nanotechnology, Hebrew University, Jerusalem, Israel*

[3]*Condensed Matter and Interfaces, Debye Institute, Utrecht University, Post Office Box 80000, 3508TA Utrecht, The Netherlands*

(Received 11 November 2008; published 28 April 2009)

Multiple energy scales contribute to the radiative properties of colloidal quantum dots, including magnetic interactions, crystal field splitting, Pauli exclusion, and phonons. Identification of the exact physical mechanism which couples first to the dark ground state of colloidal quantum dots, inducing a significant reduction in the radiative lifetime at low temperatures, has thus been under significant debate. Here we present measurements of this phenomenon on a variety of materials as well as on colloidal heterostructures. These show unambiguously that the dominant mechanism is coupling of the ground state to a confined acoustic phonon, and that this mechanism is universal.

DOI: 10.1103/PhysRevLett.102.177402 PACS numbers: 78.67.Hc, 73.21.La

The radiative properties of atoms, molecules, and mesoscopic particles are determined to a great degree by selection rules, rendering allowed transitions "bright" and disallowed transitions "dark." In atoms, the symmetry of atomic states and the spin are the only factors governing allowed transitions. However, as the quantum system becomes larger, more degrees of freedom come into play which, through coupling, can significantly modify the nature of the emitting state. A thorough understanding of these coupling mechanisms is crucial for our understanding of the radiative properties of mesoscopic systems, as well as for our ability to design systems with desired properties. Colloidal semiconductor nanocrystals are an excellent system for study of such couplings and interactions. Indeed, the size-tunable fluorescence properties of these nanocrystal quantum dots (nQDs), which are governed by quantum confinement, have been extensively scrutinized [1,2]. Aside from the basic scientific interest, the fluorescence of nQDs serves as basis for their application as fluorescent markers in biology [3] and as chromophores in electrooptic devices such as LEDs and lasing media [4].

In these systems, the lowest energy excitation is, to lowest order, multiply degenerate. This degeneracy is lifted by various physical mechanisms [5]. In particular, the e^{-}-h^{+} exchange interaction leads to the formation of a low lying dark state with total angular momentum $l = 2$ such that the ground state is effectively a dark one (for the simple case of spherical crystals with a cubic lattice). The presence of such a dark state was verified experimentally for a variety of nQD systems, including CdSe, InAs, CdTe, and PbSe. The energetic splitting of the dark state essentially manifests a $1/r^3$ scaling with the nQD radius (for more details see Ref. [1] and references therein).

A systematic study of the radiative properties at low temperatures can reveal the physical mechanisms leading to the significantly enhanced radiative rates observed at higher temperatures. This type of measurement was performed on the prototypical system of CdSe nanocrystals [6–9], revealing a significant shortening of the radiative lifetime at a temperature of about 10 K. This effect was attributed by various authors to several mechanisms, including coupling to surface states [6], exchange interaction with dangling bonds [7], and shape dependence of the band edge exciton structure [9]. In this Letter we show, by conducting experiments on several different materials and particle compositions, that the low-temperature photophysics of nQDs is governed by coupling with confined discrete acoustic phonons, and that this behavior is universal. On the other hand, there are observed differences between materials, which can provide new spectroscopic information on the ground state and its symmetry properties.

Figure 1(b) shows a set of measurements at various temperatures up to 100 K in InAs nanoparticles, whose detailed synthesis is given elsewhere [10] [a TEM image of these dots is given in Fig. 1(a)]. At $T > 20$ K a single-exponential decay is observed, while at very low temperatures this is preceded by a rapid transient emission, clearly observed in the top (4 K) curve. As can be readily seen, the radiative lifetime, manifested by the slow decay component, is on the microsecond scale, and further increases with decreasing temperatures. Similar measurements were performed using several sizes of nanoparticles, as well as on CdTe nanoparticles, synthesized according to [11] and on PbSe nanoparticles, synthesized according to [12]. The behavior observed in Fig. 1 is universal for all particle compositions and sizes, and is in good agreement with previous measurements on CdSe QDs [6–9]. The data can be attributed to emission from two states at thermal equilibrium energetically separated by ΔE. The lowest "slow" state has a longer lifetime τ_s, while the lifetime of the higher, "fast" state has a lifetime τ_f.

$$\tau^{-1} = \left(\frac{e^{\Delta E/kT}}{1 + e^{\Delta E/kT}}\right)\tau_s^{-1} + \left(\frac{1}{1 + e^{\Delta E/kT}}\right)\tau_f^{-1}. \quad (1)$$

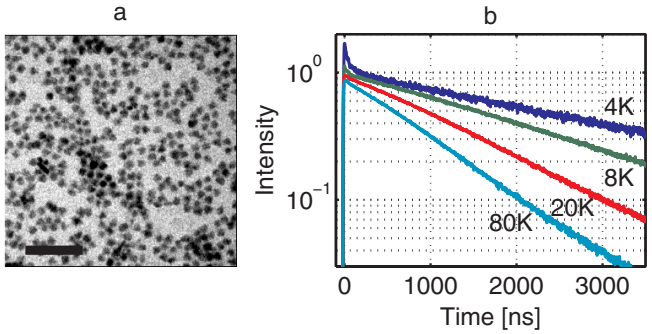

FIG. 1 (color online). (a) Transmission electron microscope image of InAs/CdSe/ZnSe nanocrystals with a core radius of 2.4 nm and a total radius of 3 nm (scale bar is 50 nm). (b) Normalized time resolved emission traces from these nanocrystals at several temperatures. A clear decrease in the (nearly single-exponential) lifetime is measured between 4 K (top) and 80 K (bottom). At low temperatures ($T \leq 10$ K) a fast transient is observed. Plots are vertically shifted for clarity.

A fit of the measured lifetime according to Eq. (1) is presented in Fig. 2(a) for two sizes of InAs QDs and in Fig. 2(b) for three sizes of PbSe QDs. For PbSe, as well as CdSe [9] and CdTe (not shown), the lifetimes become shorter with increasing size, while no such clear trend is observed for InAs. One general trend, however, is observed for all materials: The extracted ΔE clearly decreases as a function of dot size, and is in the range 0.5 meV $< \Delta E <$ 4 meV for all cases.

The origin of this energy scale is next considered. Typical energies for the exchange interaction splitting discussed above are larger by a factor of 5–10 as compared with the ΔE observed here. For example, in 2 nm radius InAs nQDs the exchange interaction is ≈ 10 meV [13]. The observed energy splittings are on the same energy scale as that of confined acoustic phonons in nQDs. The

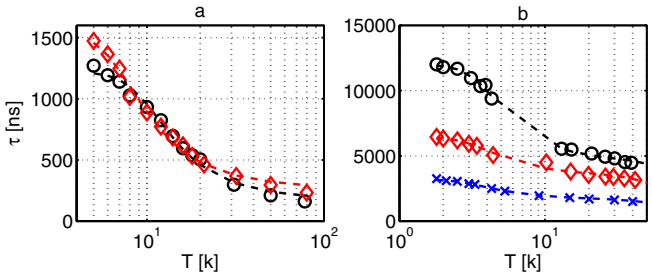

FIG. 2 (color online). The observed lifetime as a function of temperature, plotted along with fits from which ΔE is extracted (dashed lines) for various sizes of (a) InAs nanocrystals, $r =$ 1.8 nm ($\tau_s = 1.2$ μs, $\tau_f = 90$ ns, $\Delta E = 3.3$ meV circles), $r =$ 2.4 nm ($\tau_s = 1.5$ μs, $\tau_f = 130$ ns, $\Delta E = 2.2$ meV diamonds), and (b) PbSe nanocrystals, $r = 1.6$ nm ($\tau_s = 12$ μs, $\tau_f =$ 2.5 μs, $\Delta E = 1.2$ meV circles), $r = 1.8$ nm ($\tau_s = 6.5$ μs, $\tau_f = 2.0$ μs, $\Delta E = 1.0$ meV diamonds), $r = 2.15$ nm ($\tau_s =$ 3.3 μs, $\tau_f = 0.9$ μs, $\Delta E = 0.9$ meV $\times$'s).

discrete spectrum of acoustic phonons in colloidal nanocrystals can be reasonably well approximated by Lamb theory [14], assuming that the nanoparticle is an isotropic sphere with stress-free boundary conditions. Briefly, the solutions can be classified as either spheroidal or toroidal (volume maintaining) modes, and are characterized by the angular momentum they carry. The simplest solution is the $l = 0$ breathing mode, corresponding to homogeneous expansion and contraction of the entire sphere. In this case, the vibrational frequency is given by $\nu = c_L \chi / 2\pi R$, where χ is the solution of

$$\tan\chi = \frac{\chi}{1 - c_L^2 \chi^2 / (4 c_T^2)}, \tag{2}$$

and c_L and c_T are the longitudinal and transverse wave velocity in the medium, respectively. The lowest energy mode, however, belongs to a set of $l = 2$ solutions (in the simplest of which, the sphere is deformed to an oblate, then to a prolate spheroid [15]), and has an energy of approximately 40% of that of the $l = 0$ mode (for a more detailed solution see, for example, Salvador *et al.* [16]). Regardless of the details of the mode, Lamb theory solutions are characterized by a $1/r$ dependence of the discrete acoustic-phonon energy on the particle radius.

In order to establish the role of the acoustic modes in the temperature dependence of the fluorescence decay, we take advantage of the fact that in a core-shell heterostructure with a type-I band alignment (i.e., that both electrons and holes localize in the core) the electronic properties (such as the bright-dark energy splitting of the ground state exciton) depend predominantly on the core size, whereas the energy of confined acoustic phonons depends predominantly on the overall size (since the elastic properties of the shell material are close to those of the core). We therefore performed temperature-dependent lifetime measurements on core-shell/shell (CSS) InAs/CdSe/ZnSe nanocrystals [10] with core radii ranging between 1 nm and 2.8 nm, and compare these to measurements performed on core-only nanocrystals (with radii of 1.8–2.4 nm).

As can be seen from Fig. 3, the energy splitting follows a linear dependence on the inverse overall radius of the nanoparticle, as expected for an acoustic-phonon mediated process. In particular, one should note that the splitting for the 1 nm core radius CSS nanoparticle (having an overall radius of 2.5 nm) is smaller than that of the 1.8 nm radius core-only nanoparticle. This is opposite to what should have been observed for a splitting of electronic origin. In Fig. 3, we further plot acoustic-phonon energies extracted from transient absorption measurements of InAs nQDs [17], showing good agreement with the present findings, and also good agreement with the calculated energy of the $l = 0$ breathing mode (dashed line). Therefore, the data unequivocally show that the emission properties at low temperature are dominated by coupling to a discrete acoustic mode.

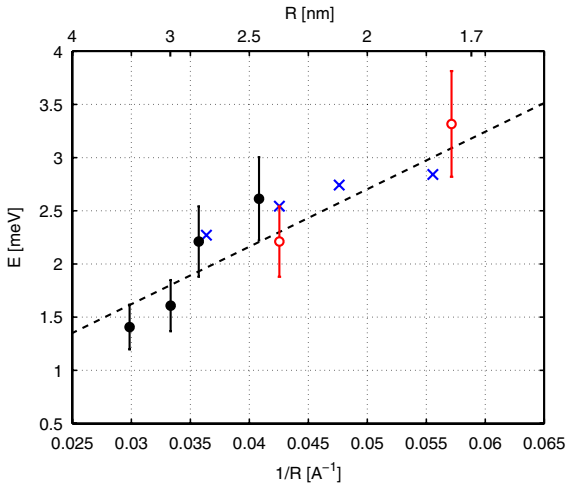

FIG. 3 (color online). The activation energy for reduction in the radiative lifetime for various sizes of core-only InAs QDs (empty red circles) and CSS InAs/CdSe/ZnSe (filled black circles) QDs as a function of the inverse overall radius of the particles. Also plotted are TA measurements (blue ×'s[17]) and the Lamb theory prediction for the $l = 0$ mode (dashed line).

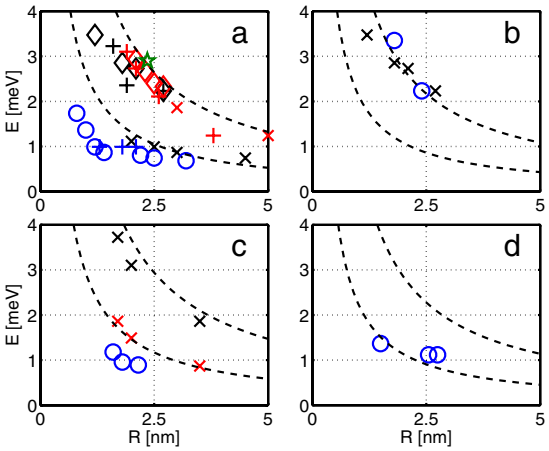

FIG. 4 (color online). Acoustic-phonon energies from temperature-dependent lifetime measurements [blue (dark gray)] as compared with those obtained from Lamb theory (dashed lines: upper is the $l = 0$ mode and lower is the lowest energy $l = 2$ mode) as well as from various other types of measurements—TA (black), Raman [red (light gray)], and spectrally resolved emission (green pentagram). Data are presented for the following: (a) CdSe (black diamonds [17], ×'s [18], crosses [19]; red crosses [21], diamonds [22], ×'s [23]; green pentagram [24]; blue crosses [7], circles [9]). (b) InAs (black ×'s [17], blue circles this work). (c) PbSe (black ×'s and red ×'s [20], blue circles this work). (d) CdTe (blue circles this work).

The universality of the assignment of the observed splitting to acoustic modes is further demonstrated in Fig. 4, which represents a large collection of such energetic splittings for different nQD systems. Also plotted are compilations of acoustic-phonon energies obtained by different measurement techniques, including transient absorption (TA) [17–20], resonant Raman spectroscopy [20–23] and emission spectroscopy [24]. We also plot simple calculations of Lamb theory for the lowest energy $l = 2$ spheroidal mode (lower dashed lines), and for the $l = 0$ spheroidal breathing mode (upper dashed lines). Elastic parameters for these cases were obtained from Refs. [12,25,26]. Note that the matrix properties have some effect on the Lamb theory predictions, not considered here [27].

Figure 4(a) presents the data on the acoustic-phonon energies derived from temperature-dependent lifetime measurements in CdSe nQDs [blue (dark gray) circles] and from a variety of techniques used to probe acoustic-phonon energies, including TA measurements (black) [17–19], Raman measurements [red (light gray)] [21–23], a spectrally resolved emission measurement (green pentagram) [24], and previous temperature resolved lifetime measurements (blue) [7,9]. All measurements seem to line up with the two modes calculated from Lamb theory.

Similar graphs, albeit with significantly less available data, are plotted in Fig. 4(b) for InAs, Fig. 4(c) for PbSe, and Fig. 4(d) for CdTe. As can be seen, the agreement between the $l = 2$ prediction from Lamb theory and ΔE extracted from the temperature-dependent lifetime measurements is good for all materials except InAs, where the measurements are in very good agreement with the $l = 0$ mode.

Phonon-mediated brightening of the exchange-splitting related dark state has been extensively observed in relation to LO phonons [1,5,6], where it was shown that the relative contribution of the 1-phonon line to the emission is significantly larger at low temperatures. Coupling of the $l = 2$ exchange-split "dark" transition to $l = 1$ or $l = 2$ acoustic modes had been considered theoretically over a decade ago [28]. Coupling to the discrete acoustic mode provides the required angular momentum to render the optical transition allowed. Indeed, our data for CdSe, CdTe, and PbSe are consistent with coupling to the spheroidal $l = 2$ acoustic mode. These results are, in fact, supported by cryogenic fluorescence line-narrowing experiments [6], where it was observed that the zero-LO-phonon line contribution to the emission (which can be acoustic-phonon assisted) dramatically increases as the temperature is increased from 1.75 to 10 K. From these results and from our current experimental findings, we assign the "slow" transition at the lowest temperature to emission from the ground (0-LO-phonon, 0-AO-phonon) vibronic state of the electronically excited state to the first LO-phonon level in the ground state (giving rise to emission redshifted by 1-LO-phonon energy). The "fast" component observed at higher temperatures is assigned to the transition from the $l = 2$ acoustic-phonon coupled electronic excited state to the 0-LO-phonon vibronic ground state (giving rise to zero-LO-phonon-line emission blueshifted by one-AO-phonon energy). It is important to note that these three materials are

of different crystal structures: wurtzite for CdSe, zinc blende for CdTe, and rock salt for PbSe. Nevertheless, the results manifest universal behavior.

The results on InAs shed some new spectroscopic light on the nature of the ground state exciton in this system. In this case, unlike CdSe, CdTe (which, like InAs has a cubic zinc blende structure), or PbSe, the ground state emission does not couple to the $l = 2$ mode, but rather the energies are consistent with the $l = 0$ breathing mode. This implies that the symmetry of the ground state optical transition is different in this case. Eight band effective mass based calculations show that for InAs the P state in the valence band is only slightly higher in energy than the S state [29]. Pseudopotential calculations predicted a P-like nature for the ground hole state [30]. The proximity between these two states is thus expected to modify the properties of the ground state optical transition, including its coupling to acoustic modes.

The presented measurements and analysis provide solid proof that other physical mechanisms invoked for description of the lifetime increase below 20 K in nQDs, involving surface states [6,7] or a (dipole induced) change in the exciton fine structure [9], are, at the very least, not dominant. Instead, coupling with confined acoustic phonons is shown to induce excitonic decay. Confined acoustic modes therefore play a significant role not only in dephasing of the electronic transition in nQDs [1,31] but also in the radiative properties of the ground state transition. The universal behavior emphasizing the central role of the discrete acoustic modes in the radiative relaxation of the nQDs is unique to these types of quantum dot systems. In embedded QDs grown, for example, by molecular beam epitaxy, there is three-dimensional electronic confinement, but there is still a continuum of acoustic modes related to the boundary conditions where the host semiconductor possesses nearly similar elastic parameters as the dots. Indeed, contrary to the nQD system, the radiative lifetime of epitaxially grown QDs is nearly temperature independent below ≈ 50 K [32].

Partial support of the Israeli Ministry of Science Tashtiyot program is gratefully acknowledged.

*banin@chem.ch.huji.ac.il

[1] U. Woggon, *Optical Properties of Semiconductor Quantum Dots* (Springer-Verlag, Berlin, 1997).
[2] D. J. Norris and M. G. Bawendi, Phys. Rev. B **53**, 16 338 (1996).
[3] M. Bruchez, M. Moronne, P. Gin, S. Weiss, and A. P. Alivisatos, Science **281**, 2013 (1998).
[4] V. I. Klimov *et al.*, Science **290**, 314 (2000).
[5] M. Nirmal, D. J. Norris, M. Kuno, M. G. Bawendi, Al. L. Efros, and M. Rosen, Phys. Rev. Lett. **75**, 3728 (1995); Al. L. Efros, M. Rosen, M. Kuno, M. Nirmal, D. J. Norris, and M. G. Bawendi, Phys. Rev. B **54**, 4843 (1996).
[6] M. Nirmal, C. B. Murray, and M. G. Bawendi, Phys. Rev. B **50**, 2293 (1994).
[7] S. A. Crooker, T. Barrick, J. A. Hollingsworth, and V. I. Klimov, Appl. Phys. Lett. **82**, 2793 (2003).
[8] O. Labeau, P. Tamarat, and B. Lounis, Phys. Rev. Lett. **90**, 257404 (2003).
[9] C. de Mello Donega, M. Bode, and A. Meijerink, Phys. Rev. B **74**, 085320 (2006).
[10] A. Aharoni, T. Mokari, I. Popov, and U. Banin, J. Am. Chem. Soc. **128**, 257 (2006).
[11] S. F. Wuister, I. Swart, F. van Driel, S. G. Hickey, and C. de Mello Donega, Nano Lett. **3**, 503 (2003).
[12] A. J. Houtepen, R. Koole, D. Vanmaekelbergh, J. Meeldijk, and S. G. Hickey, J. Am. Chem. Soc. **128**, 6792 (2006).
[13] U. Banin, J. C. Lee, A. A. Guzelian, A. V. Kadavanich, and A. P. Alivisatos, Superlattices Microstruct. **22**, 559 (1997).
[14] H. Lamb, Proc. London Math. Soc. **s1-13**, 189 (1881).
[15] L. Saviot and D. B. Murray, Phys. Rev. B **72**, 205433 (2005).
[16] M. R. Salvador, M. W. Graham, and G. D. Scholes, J. Chem. Phys. **125**, 184 709 (2006).
[17] G. Cerullo, S. De Silvestri, and U. Banin, Phys. Rev. B **60**, 1928 (1999).
[18] P. Palinginis, S. Tavenner, M. Lonergan, and H. Wang, Phys. Rev. B **67**, 201307(R) (2003).
[19] D. M. Sagar, R. R. Cooney, S. L. Sewall, E. A. Dias, M. M. Barsan, I. S. Butler, and P. Kambhampati, Phys. Rev. B **77**, 235321 (2008).
[20] M. Ikezawa, T. Okuno, Y. Masumoto, and A. A. Lipovskii, Phys. Rev. B **64**, 201315(R) (2001).
[21] L. Saviot, B. Champagnon, E. Duval, I. A. Kudriavtsev, and A. I. Ekimov, J. Non-Cryst. Solids **197**, 238 (1996).
[22] U. Woggon, F. Gindele, O. Wind, and C. Klingshirn, Phys. Rev. B **54**, 1506 (1996).
[23] M. J. Fernee, B. N. Littleton, S. Cooper, H. Rubinsztein-Dunlop, D. E. Gomez, and P. Mulvaney, J. Phys. Chem. C **112**, 1878 (2008).
[24] G. Chilla *et al.*, Phys. Rev. Lett. **100**, 057403 (2008).
[25] E. Deligoz, K. Colakoglu, and Y. Ciftci, Physica (Amsterdam) **373B**, 124 (2006).
[26] Yu. A. Burenkov, S. Yu. Davydov, and S. P. Nikanorov, Sov. Phys. Solid State **17**, 1446 (1975).
[27] L. Saviot, D. B. Murray, and M. del Carmen Marco de Lucas, Phys. Rev. B **69**, 113402 (2004).
[28] Al. L. Efros, Phys. Rev. B **46**, 7448 (1992).
[29] U. Banin *et al.*, J. Chem. Phys. **109**, 2306 (1998).
[30] A. J. Williamson and A. Zunger, Phys. Rev. B **61**, 1978 (2000).
[31] A. Vagov, V. M. Axt, T. Kuhn, W. Langbein, P. Borri, and U. Woggon, Phys. Rev. B **70**, 201305(R) (2004).
[32] G. Wang, S. Fafard, D. Leonard, J. E. Bowers, J. L. Merz, and P. M. Petroff, Appl. Phys. Lett. **64**, 2815 (1994); H. Yu, S. Lycett, C. Roberts, and R. Murray, Appl. Phys. Lett. **69**, 4087 (1996).